Microbiome

RESEARCH

Open Access

# Soil warming increases the active antibiotic resistome in the gut of invasive giant African snails

Yiyue Zhang[1,2†], Hong-Zhe Li[1,2†], Martin Breed[3], Zhonghui Tang[1,4], Li Cui[1,2,5], Yong-Guan Zhu[1,2,5,6] and Xin Sun[1,2,5*]

## Abstract

**Background** Global warming is redrawing the map for invasive species, spotlighting the globally harmful giant African snail as a major ecological disruptor and public health threat. Known for harboring extensive antibiotic resistance genes (ARGs) and human pathogens, it remains uncertain whether global warming exacerbates these associated health risks.

**Methods** We use phenotype-based single-cell Raman with $D_2O$ labeling (Raman-$D_2O$) and genotype-based metagenomic sequencing to investigate whether soil warming increases active antibiotic-resistant bacteria (ARBs) in the gut microbiome of giant African snails.

**Results** We show a significant increase in beta-lactam phenotypic resistance of active ARBs with rising soil temperatures, mirrored by a surge in beta-lactamase genes such as SHV, TEM, OCH, OKP, and LEN subtypes. Through a correlation analysis between the abundance of phenotypically active ARBs and genotypically ARG-carrying gut microbes, we identify species that contribute to the increased activity of antibiotic resistome under soil warming. Among 299 high-quality ARG-carrying metagenome-assembled genomes (MAGs), we further revealed that the soil warming enhances the abundance of "supercarriers" including human pathogens with multiple ARGs and virulence factors. Furthermore, we identified elevated biosynthetic gene clusters (BGCs) within these ARG-carrying MAGs, with a third encoding at least one BGC. This suggests a link between active ARBs and secondary metabolism, enhancing the environmental adaptability and competitive advantage of these organisms in warmer environments.

**Conclusions** The study underscores the complex interactions between soil warming and antibiotic resistance in the gut microbiome of the giant African snail, highlighting a potential escalation in environmental health risks due to global warming. These findings emphasize the urgent need for integrated environmental and health strategies to manage the rising threat of antibiotic resistance in the context of global climate change.

**Keywords** Active antibiotic resistome, Antimicrobial resistance, Soil warming, Single-cell Raman spectroscopy, Human bacterial pathogen

†Yiyue Zhang and Hong-Zhe Li contributed equally to this work.

*Correspondence:
Xin Sun
xsun@iue.ac.cn
Full list of author information is available at the end of the article

## Introduction

Global climate change is causing soil warming, which has enduring and complex impacts on terrestrial ecosystems [1–3]. While substantial research has been done on the impact of soil warming on microbial communities [4, 5], little is known about the impacts of warming on soil fauna and potential feedbacks to soil microbial communities [6]. Rising temperatures are closely linked to both physiological and behavioral changes in soil fauna, ranging from metabolic rate adjustments to altered reproductive behaviors [7, 8]. Moreover, the gut of soil fauna represents a hidden reservoir of soil microbiomes, including antibiotic resistomes (the collection of all the antibiotic resistance genes) [9] and pathogenic microorganisms [10, 11]. Soil warming may disrupt host-microbiome interactions, potentially facilitating the emergence of new pathogens and increasing risks of exposure to infectious disease causing agents [12, 13]. This is particularly relevant for ectothermic fauna, as they are inherently thermo-sensitive and which can cause gut microbiome changes [14]. However, the specific impact of soil warming on the gut microbiome of ectothermic fauna remains poorly understood. The nexus between antimicrobial resistance (AMR) and pathogenic microorganisms within the gut of soil fauna under changing temperatures is of paramount importance, especially considering the global urgency in managing antibiotic resistomes [15, 16] and climate change impacts.

The giant African snail (*Achatina fulica*) is an invasive species of global importance and is known to harbor a diverse and highly abundant collection of antibiotic resistant genes (ARGs) and human pathogens, presenting ecosystem and health risks [11]. These snails have proliferated in many tropical and subtropical ecosystems, and display exceptional adaptability and survival capabilities [17]. They are typically nocturnal, being most active during cooler night hours and seeking refuge in the soil during the day [18]. This soil-dwelling behavior makes them particularly susceptible to changes in soil temperature. As global warming progresses, increasing soil temperatures are expected to elevate the environmental risks associated with these snails. It is crucial to consider the potential for changes in the gut microbiome and resistome patterns in these snails. Thus, the giant African snail serves as an ideal model organism for investigating the impacts of soil warming on the pathogenic microorganisms and AMR in the gut microbiome of soil ectothermic fauna under climate change conditions.

Recent advancements in high-throughput PCR and sequencing technologies have enabled the detailed study of the microbiome and resistome of soil fauna. For instance, metagenomics can detail the complex bacterial communities within the gut of earthworms, revealing a rich array of ARGs that reflect soil health and environmental exposures [19, 20]. Genetic techniques primarily yield inferred insights into antibiotic-resistant bacteria (ARBs), but are limited by the challenge of distinguishing genes from active cells, dead cells, and/or extracellular DNA [21, 22]. Thus, it is important to investigate active ARBs to better assess the risks posed. Traditional culture-based techniques are also limited by only characterizing culturable bacteria and > 95% of soil bacteria are unculturable, leading to a bias in the study of active ARBs in in situ environments. A phenotypic approach that integrates single-cell Raman spectroscopy with heavy water labeling (Raman-$D_2O$) can overcome this limitation, where this technique has demonstrated promise in identifying active ARBs in a culture independent way [23, 24]. Notably, Raman-$D_2O$ has been used for ARB detection in diverse environments, including soils, rivers, and the human gut [21, 25], revealing the effects of human activities on active ARBs. Combining single-cell Raman technology with metagenomic sequencing is thus a powerful approach to explore ARBs at both the genotypic and phenotypic levels. This integrative approach provides a comprehensive understanding of active ARBs and enables a detailed analysis of ARBs, which we use here to study the resistome from within the gut of soil fauna under experimentally altered temperatures.

While extensive studies have reported the effects of climate warming on soil microbial functions, research on microbial biosafety, particularly concerning AMR in the context of climate change, remains relatively scarce. Our study addresses this challenge by focusing on AMR in invasive ectothermic fauna, using soil warming as an environmental change factor. We employed an integrative approach combining single-cell Raman-$D_2O$ technology with metagenomics to explore the active ARBs as well as pathogenic microorganisms within the gut microbiome of the giant African snail across experimentally variable soil temperatures. Additionally, we investigate biosynthetic gene clusters (BGCs)—groups of adjacent genes coordinating the production of secondary metabolites—which play a crucial role in microbial adaptation and competition. We hypothesize that elevated temperatures will influence the antibiotic resistance mechanisms within these microbial communities and increase the activity of ARB and their associated pathogenic microorganisms in the gut microbiome of the giant African snail. Our study offers a new window into how global warming may accelerate the emergence and spread of AMR.

## Methods

### Experimental design

We collected > 80 wild eggs from a single giant African snail in an urban setting in Xiamen City, China (Fig. 1A),

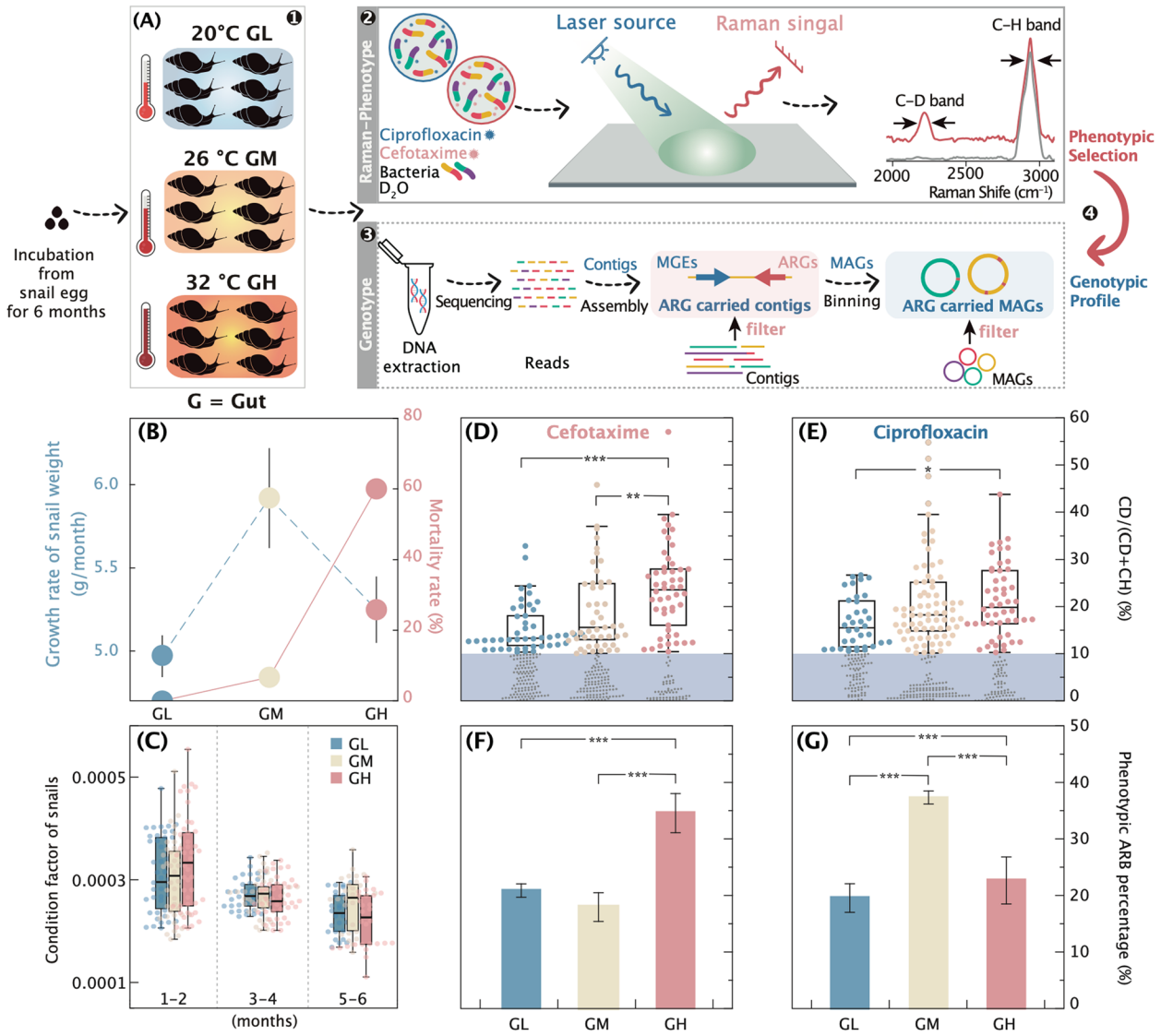


**Fig. 1** Experimental design, life-history traits, and phenotypic resistance traits. **A** Schematic of the experimental design and working flow. **B** Snail growth rate (left *y*-axis) and mortality rate (right *y*-axis). **C** Condition factor metrics for snails. **D**–**E** The C-D ratio (CD/[CD + CH]) in single-cell gut bacteria under treated with two antibiotics. **F**–**G** The percentage of phenotypic antibiotic-resistance bacteria (ARB) under treated with two antibiotics, compared across various temperature groups. Comparison between the two types of samples was analyzed with Wilcoxon signed-rank test. ns, non-significant; *$p < 0.05$; **$p < 0.01$; ***$p < 0.001$. Non-significant differences between sample types in some ARG types were not labeled. The samples are designated as follows: snail gut microbiome samples (G) under low (GL, 20 °C), medium (GM, 26 °C), and high (GH, 32 °C) temperature treatments

ensuring genetic consistency across the study and minimizing potential confounding factors. Our previous study has thoroughly documented the habitat and biological contamination characteristics of the giant African snail [11]. These eggs were initially incubated under natural, ambient conditions until hatching, which occurred within 10 days. After hatching, the newly hatched snails were transferred to incubators set at different temperatures: low (20 °C), medium (26 °C), and high (32 °C). The 20 °C treatment serves as our lower baseline, closely representing the average nighttime temperature in Xiamen from April to October, which matches the location and timing of when we did the study. While giant African snails can withstand a wide range of temperatures (0 to 45 °C), their optimal growth and activity occur between 20 and 32 °C [26]. Temperatures outside this range induce dormancy [26]. The incubators maintained a 14/10-h photoperiod and a constant 60% relative humidity. Each

hatchling was placed in a sterilized 20 × 20 × 10-cm plastic culture box with 200 g of sterile, balanced loam soil for the 6-month duration of the experiment. Soil sterilization and physicochemical property evaluation ensured that it was free of contaminants and suitable for snail development.

We recorded growth and mortality parameters, including snail weight (g) and shell length (mm) during incubation. A total of 45 snails (15 from each temperature group) were selected for detailed analysis of shell length, weight, and other parameters. Shell length data were accurate to the nearest 0.5 mm, and weights to the nearest 0.001 g. We used the condition factor (weight/shell length)^3 as a condition indicator of individual snail health [27]. After incubation and a 48-h fasting period, we recorded feces weights and divided the fecal samples into three: one for antibiotic-resistant phenome analysis, one for DNA extraction, and one stored at − 80 °C. We collected soil samples from each incubator, which were pooled from sampling at five points within incubators to create a representative sample for downstream analysis.

#### *Resistant phenome discrimination of gut bacteria* via *Raman-$D_2O$ labeling*

Following incubation, we collected freshly excreted snail feces and subjected them to a 16-h desiccation process to eliminate excess moisture (Fig. 1A). For the deuterium isotope labeling approach, we mixed 1 g of the dried fecal matter with 100 µL of $D_2O$ (99% atom % D, Sigma-Aldrich) and 100 µL of antibiotic solution, incubating for 24 h at their respective temperatures consistent with our previous findings [21]. We used cefotaxime and ciprofloxacin (from McLean, Shanghai, China) for resistance phenotyping, with effective doses set at 10 × MIC and 100 × MIC, respectively [21]. Each antibiotic solution was sterilized through 0.22-µm filters (Millipore Millex, USA) and stored at − 20 °C until use. We isolated gut microbiomes using the Nycodenz density-gradient separation method [21]. Briefly, 1 g of feces was mixed with 5 mL of 0.02% Tween 20 in phosphate-buffered saline (PBS) and vortexed vigorously for 30 min. This mixture was then combined with 5 mL of 0.8 g/mL Nycodenz solution (≥ 98%, Aladdin) and centrifuged at 10,000 rcf for 60 min. We collected the intermediate layer post-centrifugation, transferring it to a sterile tube and rinsing thrice with deionized water to remove residual PBS.

#### Single-cell Raman spectra procurement and data analysis

We placed bacteria derived from feces on aluminum-coated slides (HOOKE Instruments Ltd., China) and air-dried them at room temperature prior to Raman measurements. Using a LabRAM Aramis confocal Raman microscope (HORIBA Jonin-Yvon, Japan) equipped with a 532-nm Nd:YAG laser (Laser Quantum) and a 300 g/mm grating, we collected single-cell Raman spectra. The laser power at the sample was set to 3.5 mW. An Olympus × 100 objective (Japan) was utilized to capture Raman signals, with each cell requiring a 15-s acquisition time. Before analyzing the Raman data, we evaluate the signal-to-noise ratio of all spectra and remove Raman spectra with a high level of visible noise. This serves as a quality control measure for the data. Raman spectroscopy is a single-cell level detection method that reflects bacterial heterogeneity. Therefore, any Raman data with a high signal-to-noise ratio will be included in the analysis.

Spectra, acquired in the 500–3200 $cm^{-1}$ range, facilitated the calculation of the CD/(CD + CH) ratio, representing cellular deuterium (D) assimilation. This was achieved by integrating spectral regions corresponding to C-D (2040–2300 $cm^{-1}$) and C-H vibrations (2800–3100 $cm^{-1}$). We collected over 600 Raman spectra from each soil sample to estimate the abundance of D-labeled bacteria. The percentage of ARB was calculated as the count of D-labeled bacteria identified by Raman-$D_2O$, divided by the total number of detected single cells. The phenotypic resistance level was determined by multiplying the ARB percentage by activity. To minimize the influence of fecal nutrition levels on deuterium incorporation, C-D ratios were normalized using a control from an antibiotic-free fecal sample. The threshold for active cell labeling was set at 0.1, calculated as the mean plus three standard deviations of normalized C-D ratios in D-free bacteria. More than 200 single cells from each fecal sample were measured.

#### DNA extraction and 16S rRNA amplicon sequencing

Approximately 0.25 g of both fecal and soil samples were used for total genomic DNA extraction, using the FastDNA Spin Kit for Soil (MP Biomedicals, USA). The quality of the extracted DNA was assessed using a NanoDrop 2000 Spectrophotometer (Thermo Scientific, USA), with absorbance ratios at A260/280 (approximately 1.8) and A260/230 (> 1.7), indicating satisfactory purity. Precise DNA quantification was performed using the Qubit 3.0 Fluorimeter (Thermo Scientific, USA) with fluorescence detection. Following DNA extraction and assessing quality, we amplified 16S rRNA gene fragments from fecal and soil samples using quantitative PCR with 515F-907R primers, adhering to Environmental Microbiology Minimum Information (EMMI) guidelines [28]. Sequencing was conducted on the Illumina MiSeq PE300 platform (Majorbio, Shanghai, China), employing 2 × 300 bp paired-end libraries. Read processing was carried out using Usearch (v.11.0) and subjected to de-noising using the DADA2 pipeline [29] and QIIME2 [30]. After quality trimming and chimera removal, we

generated an abundance table of amplicon sequence variants (ASVs) with 100% sequence similarity for 16S rRNA genes. The taxonomic assignment of the remaining sequences was performed using the RDP classifier within the SILVA database (release 138).

#### Metagenome sequencing, assembly, and binning

Paired-end sequencing (2 × 150 bp) of DNA was conducted on the Illumina NovaSeq 6000 platform (Illumina Inc., San Diego, CA, USA), utilizing NovaSeq Reagent Kits and following the manufacturer's instructions. After sequencing, the data underwent rigorous quality assessment using FastQC (v0.11.5) [31], followed by refinement with Trimmomatic (v0.33) [32], and host sequence decontamination was performed using Bowtie2 (v2.2) [33]. This process yielded a total of 257 Gb of clean metagenome sequences, with each of the 28 samples providing at least 11 Gb. For the binning process, MetaWRAP (v1.2.1) [34] was employed, utilizing three methodologies: CONCOCT (v0.4.0) [35], MaxBin (v2.2.2) [36], and MetaBAT2 (v2.12.1) [37]. The bin_refinement module from MetaWRAP was then used to consolidate the binning results from these three approaches to recover a single and improved bin set. The quality of the metagenome-assembled genomes (MAGs) was assessed using CheckM (v1.2.0) [38], with retention criteria set at ≥ 90% completeness and ≤ 10% contamination. Taxonomic affiliations for each MAG were determined using GTDB-Tk (v2.3.0) classify_wf, with the R214 database [39]. Phylogenetic analysis of the MAGs was conducted with FastTree (v2.1.10) [40], based on a selected set of 120 bacterial domain-specific marker genes from GTDB. The resulting phylogenetic tree was visualized using iTOL [41]. Secondary metabolite biosynthetic gene clusters (BGCs) were identified in the high-quality MAGs and isolated pure strains using antiSMASH (v6.1) [42], while contigs > 5 kb were examined under strict settings to exclusively detect well-defined clusters with all requisite components.

#### Resistant genotypes and identifying ARG hosts

The ARGs-OAP pipeline (v3.2) was used to process the trimmed paired-end reads under default settings, marking the initial step in annotating ARG profiles for ARG quantification. The cut-off parameters set for ARGs included alignment lengths > 75 nucleotides, an e-value < $10^{-7}$, and identities > 80% [43]. ARG abundances were normalized based on both the ARG reference sequence length and cell count derived from metagenomic datasets, with the final representation being expressed as "ARG copy per cell," following previous recommendations [44]. Annotation of ARG-carrying MAGs and contigs was conducted using the Structured Antibiotic Resistance Gene database (SARG v3.2) [34]. ORFs located on contigs with ARGs were annotated by comparison against the non-redundant (NR) protein database from NCBI (data as of 26 July 2020) [45] using the BLASTP tool, applying an E-value threshold of < $10^{-7}$. Mobile genetic elements (MGEs) carried by resistance contigs were identified using string matches from the NR annotation results. A positive co-occurrence between ARGs and MGEs was identified when an ARG was situated within a span of 10 open reading frames, either preceding or following an MGE, on the identical contig [46]. To link ARGs to specific taxonomies, assembled contigs and reconstructed microbial genomes from sequenced reads were analyzed using co-located phylogenetic biomarkers [47].

#### Isolation of ARB and MIC determination

ARBs were isolated from snail fecal samples using selective culturing techniques. Samples were plated on Luria–Bertani (LB) agar containing cefotaxime (4 μg/mL) or ciprofloxacin (1 μg/mL), with concentrations based on CLSI breakpoints for Enterobacterales [48, 49]. Morphologically distinct colonies were purified and identified using 16S rRNA gene sequencing. The minimum inhibitory concentrations (MICs) for cefotaxime and ciprofloxacin were determined using the broth microdilution method, following CLSI guidelines [48, 49]. Detailed procedures are provided in the Supplementary Information.

#### Statistical analysis

Pearson's correlation coefficient ($r$) was computed to assess the relationships between resistance phenotypes and species/genotypes, utilizing the cor.test() function in R 4.12 (R Core Team, 2020) [50]. The microeco and ggplot2 packages in R facilitated the execution of microbial alpha and beta diversity analyses, encompassing the calculation of the alpha index and the conduct of principal coordinates analysis (PCoA) [51]. One-way analysis of variance (ANOVA) was employed to analyze overall mean differences, and Tukey's honestly significant difference (HSD) test was used to identify differences between groups, establishing a $p$-value threshold of < 0.05 for significance. Analysis of similarities (ANOSIM), grounded on sample distances, was applied to evaluate differences in community ARG composition. The Kruskal–Wallis test, with Dunn's post hoc test, was used to identify differences between groups. For comparisons involving two groups, the Mann–Whitney $U$ test was employed.

## Results

#### Warming impacted active ARBs in snail gut microbiomes

We observed that snails grew least well at 32 °C compared to 20 °C and 26 °C (Fig. 1B–C). During the initial growth

phase of 1–2 months, snails in the 32 °C treatment exhibited faster growth and higher metabolic rates than those at 20 °C and 26 °C (Fig. 1C). However, at the 4–6-month stage, snails in the 32 °C group experienced a significant rise in mortality (60%; Fig. 1B). This period also corresponded with reduced growth rates (Fig. 1B) and a decline in snail condition (Fig. 1C). Single cell Raman-$D_2O$ was used to identity active ARB under ciprofloxacin and cefotaxime addition. We found that soil warming significantly increased the phenotypic resistance level of the abundance of active ARB and resistance ability of ARB to antibiotic stress. A noted escalation in C-D ratios at 32 °C for both antibiotic treatments ($p < 0.05$) signaled heightened ARB activity in the higher temperature treatment (Fig. 1D–E).

The proportion of active ARB relative to the entire population serves as an indicator to gauge ARB risk. Distinct variations were observed in this ratio across the two antibiotic settings (Fig. 1F–G). To illustrate this, the cefotaxime (beta-lactams) treatment yielded a significantly higher abundance of active ARB (34%) at 32 °C, as compared to 26 °C (17%) and 20 °C (20%) groups ($p < 0.01$, Fig. 1F). Conversely, the ciprofloxacin (quinolone) treatment manifested the highest abundance of active ARB at 26 °C (37%), which was higher than in the 32 °C (22%) and 20 °C (19%) treatment groups ($p < 0.01$, Fig. 1G). Overall, higher temperatures generally amplified the activity and abundance of ARB.

#### Warming shifted the composition of microbiomes

Temperature treatments had a significantly impact on the composition of both gut and soil bacterial communities (Fig. 2). The relative abundance of the predominant genera showed marked variability across temperature groups with notable differences in their temperature-related trajectories (Fig. 2A). Among the most abundant genera, both *Klebsiella* and *Microbacterium* displayed significant increases ($p < 0.05$) in relative abundances in the higher temperature treatments, in contrast to the patterns in *Citrobacter* which had lower relative abundances in the higher temperature treatments (Fig. 2A–B). In addition, *Lactococcus* showed a peak in abundance at 26 °C, whereas the relative abundance of *JG30-KF-CM45* appeared unaffected by temperature treatments (Fig. 2B). Elevated temperatures had a positive effect on the relative prevalence of *Microbacterium* in the microbiomes of snail gut and soil samples. The relative abundance of family-level bacterial taxa also varied by temperature treatments (Fig. 2C). Consistent with these observations, a parallel trend was observed in Enterobacteriaceae in the gut microbiome samples; this bacterial lineage is closely associated with ARBs, and its relative abundance increased with increased temperatures (Fig. 2C).

Bacterial richness (Fig. S1) and Shannon index did not differ among temperature groups for either soil or snail gut samples (Fig. 2D; $p > 0.01$). The soil microbiome exhibited higher diversity than the snail gut, but lower diversity than the soil control group (Fig. 2D). A principal coordinate analysis (PCoA) revealed that the 32 °C treatment group formed a distinct cluster and 20 °C and 26 °C temperature groups showed partially overlap (Fig. 2E; $p = 0.001$, PERMANOVA with Adonis test). Furthermore, an increase in within-group variation in both soil and gut samples was observed with increasing temperature (Fig. S2; $p = 0.001$, PERMANOVA with ANOSIM test). Bacterial communities from the 20 °C and 26 °C temperature groups were clearly clustered according to compartment based on average Bray–Curtis distances of taxonomic composition at the family level across temperature treatments (Fig. S3).

#### Genotypic resistance in snail gut microbiomes

We obtained 257 Gb of clean reads that were assembled into 10,418,011 contigs with an average length of 1244 bp (Table S1). We elucidated 21 distinct ARG types, further stratified into a total of 591 ARG subtypes (Table S2). The snail gut microbiome contained 315 ARG subtypes across all ARG types, contrasting with the more extensive range of 384 subtypes found in soil samples. Beta-lactam emerged as the most diverse ARG type, represented by 84 and 120 subtypes in the snail gut and soil, respectively. Notwithstanding lower ARG diversity, the snail gut samples had elevated relative abundance of ARG (5.98 copy/cell); with an approximate 13-fold increase compared to the soil samples (0.45 copy/cell, Fig. 3A). Multidrug-resistant genes predominated in the snail gut, constituting 55% of the total, followed by unclassified (14%), macrolide lincosamide streptogramin (MLS, 6%), beta-lactam (4%), and bacitracin (4%) resistance genes (Fig. S4). In soil, ARG types exhibited a broader dispersion, with multidrug (25%), vancomycin (14%), sulfonamide (13%), tetracycline (10%), and rifamycin (6%) resistance genes being the most prevalent (Fig. S4).

In our genotype-based analysis of the antibiotic resistome in snail gut and soil samples at various temperatures, we observed distinct changes, particularly in the 32 °C groups (Fig. S5, ANOSIM $R = 0.94$, $p = 0.0002$), which mirrored shifts in microbial community patterns (Fig. 2E). The relative abundance of all (Fig. 3A), multidrug (Fig. 3B), and beta-lactam (Fig. 3C) resistance genes was robust across temperature treatments in the snail gut ($p > 0.05$, ANOVA). However, resistance genes for quinolones (Fig. 3D), tetracyclines, vancomycin, sulfonamides, rifamycin, aminoglycosides, and trimethoprim exhibited significant temperature-dependent fluctuations ($p < 0.05$, ANOVA, Fig. S6). Although multidrug

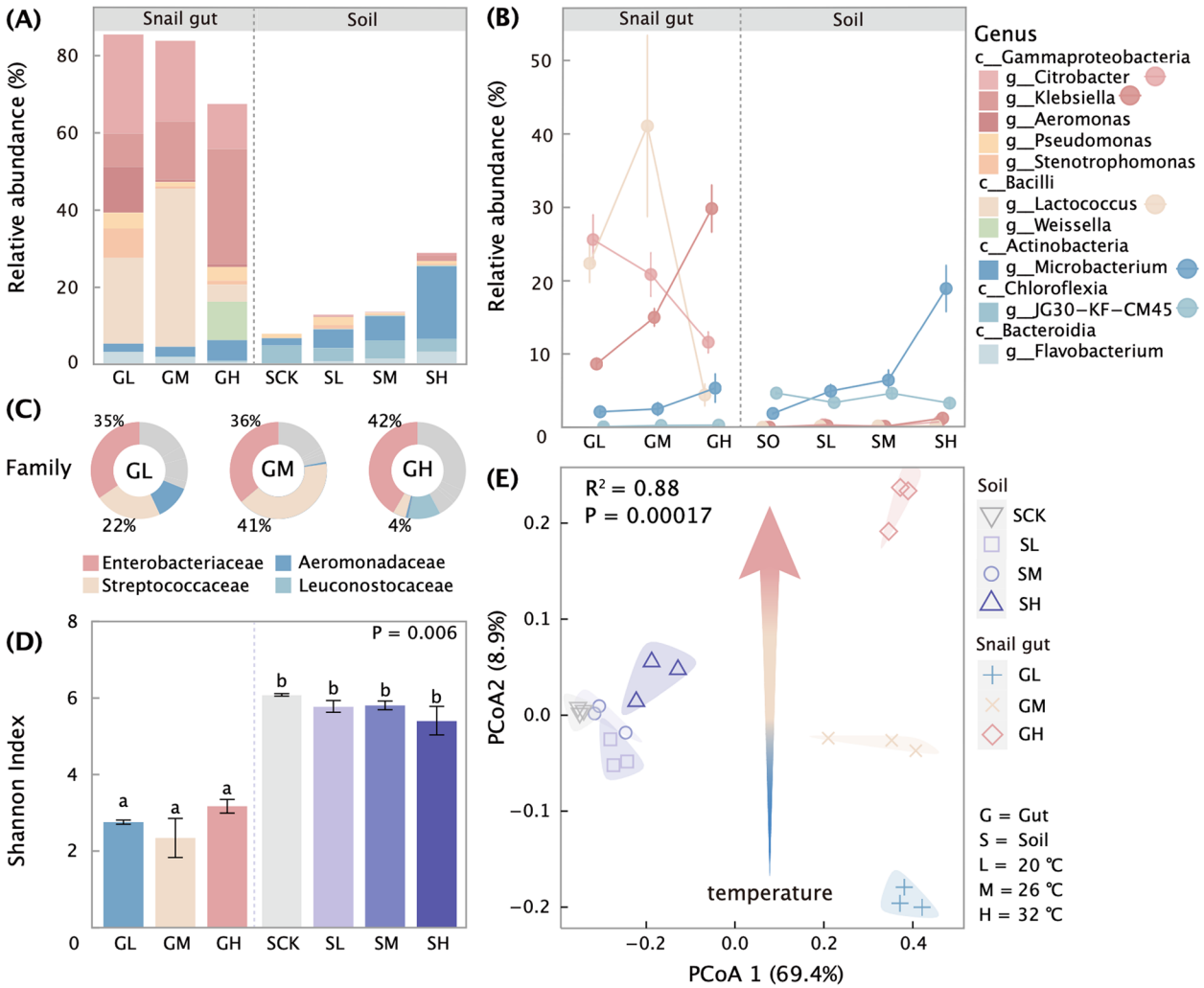


**Fig. 2** Impact of temperature on the composition and structure of gut and soil microbiomes. **A** Bar plot depicts the proportion of the top 10 bacterial genera. **B** Dotted line plots of dominant species (genus level) trends. **C** Pie chart of gut microbial composition (family level). **D** Shannon index. **E** Bray–Curtis-based PCoA of the snail gut and soil microbiome across various temperature groups. The *p*-value was based on Adonis. In panels **D** and **E**, bars with different letters indicate significant differences as defined by one-way ANOVA with Tukey's HSD test ($p < 0.05$). The samples are designated as follows: soil samples (S) and snail gut microbiome samples (G) under low (L, 20 °C), medium (M, 26 °C), and high (H, 32 °C) temperature treatments, alongside a control (CK)

and beta-lactam resistance genes displayed high diversity, their overall abundance did not show clear temperature effects (Fig. 3B–C), suggesting a masking effect that could obscure the responses of specific ARG subtypes to temperature variations. Importantly, we identified significant increases in the combined prevalence of specific beta-lactamase subtypes (SHV, TEM, OCH, OKP, and LEN) under 32 °C conditions (Fig. 3E). Collectively, these subtypes increased approximately 20-fold at 26 °C and 60-fold at 20 °C, highlighting pronounced temperature-dependent changes in these subtypes (Fig. 3E).

### Host bacteria of identified ARGs

We identified 1114 metagenome contigs as ARG-carrying contigs, housing 1188 ARGs, of which 69.2% were ascribed to multidrug resistance, and 10.6% as beta-lactam (Fig. S7). An initial analysis showed that ARG-carrying contigs were present in a phylogenetically diverse range of bacterial families (Fig. S7 and S8), including Enterobacteriaceae (36.6%), Pseudomonadaceae (8.5%), Xanthomonadaceae (4.4%), Flavobacteriaceae (3.6%), and Moraxellaceae (3.5%). Enterobacteriaceae emerged as the primary host of ARG-carrying contigs, with 35.4% genes resistant to multidrug, beta-lactam (54.8%), bacitracin (80.0%), and quinolone (29.4%) found within this lineage.

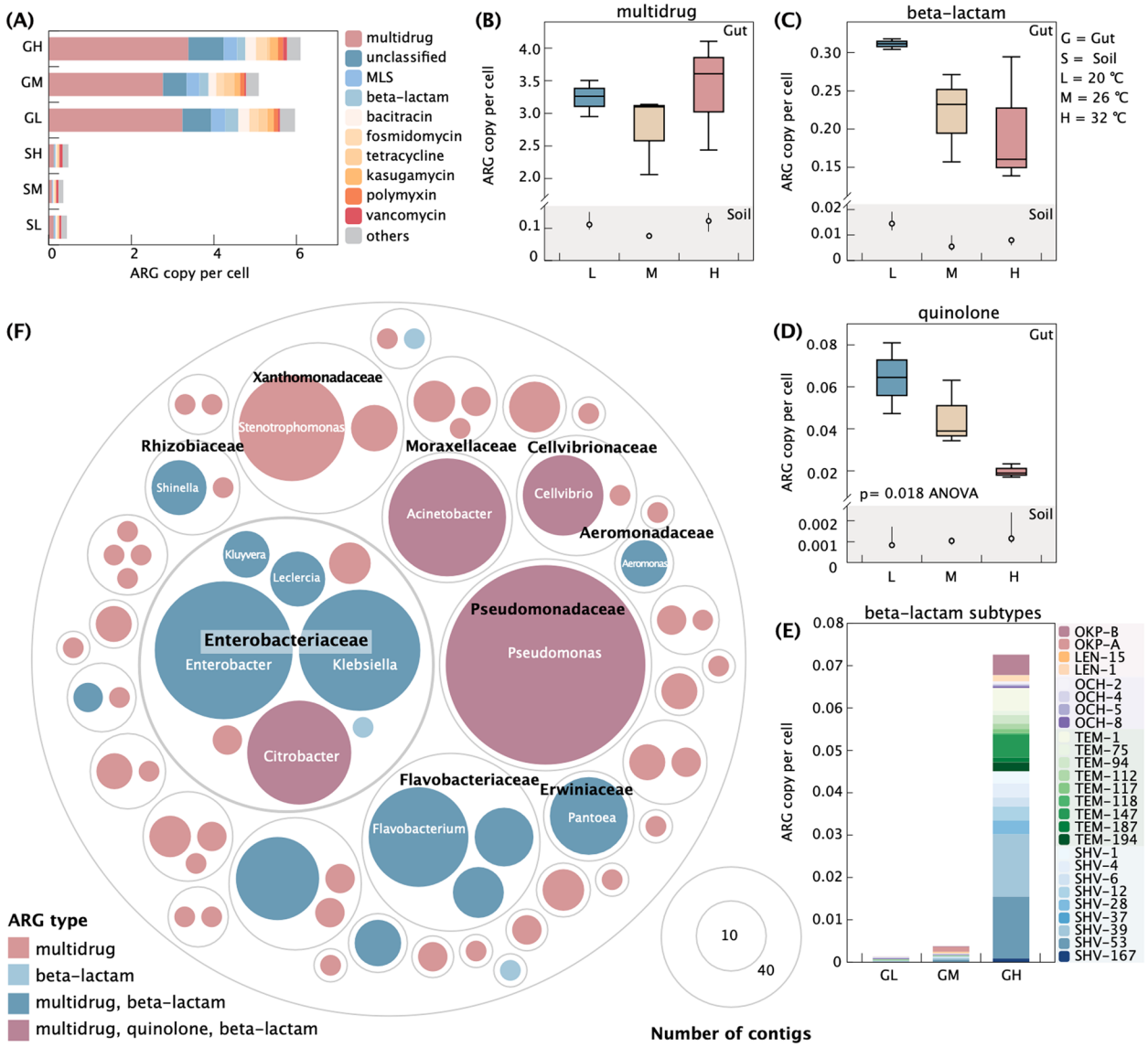


**Fig. 3** Comparison of antibiotic resistance gene (ARGs) profiles and ARGs host in snail gut and soil under different temperature treatments. **A** The abundance of total ARGs in snail gut and soil samples. **B**–**D** The abundance for multidrug, beta-lactam, and quinolone resistance types, respectively. The abundance was normalized into copy of ARGs per cell. **E** Genus-level ARG hosts depicted on contig-level resolution, with circle size proportional to contig number and color representing ARG type. The samples are designated as follows: soil samples (S) and snail gut microbiome samples (G) under low (L, 20 °C), medium (M, 26 °C), and high (H, 32 °C) temperature treatments, alongside a control (CK)

Here, we focused specifically on the genotypes of ARGs associated with multidrug, beta-lactam, and quinolone resistance, aiming to establish clearer correlations with resistance phenotype for cefotaxime (a beta-lactam) and ciprofloxacin (a quinolone). We identified 442 ARG-carrying contigs classified to the genus level that carried one or more resistance genes to multidrug, beta-lactam, and quinolone (Fig. 3F).

At the genus level, *Pseudomonas* (20.4%) emerged as the most dominant host of ARG-carrying contigs followed by *Enterobacter* (9.8%). These genera, along with *Klebsiella*, *Aerobacter*, *Stenotrophomonas*, and *Citrobacter*, collectively accounted for a significant portion (49.1%) of the total ARG diversity and harbored a wide array of targeted ARG subtypes (Table S3). Notably, beta-lactam resistance genes and their host bacteria were more abundant than their quinolone-resistant counterparts (Fig. 3F). *Pseudomonas* constituted 22.8% of the multidrug resistance, 3.5% of beta-lactam resistance, and 33.3% of quinolone resistance was observed. Conversely,


**Fig. 4** Association between genera and phenotypic antibiotic resistance in the snail gut microbiome. The left panel presents a correlation between the abundance of antibiotic-resistant bacteria (ARB) exhibiting active resistance phenotypes and the relative abundance of microbial genera (statistical significance indicated by $*p < 0.05$). The presence of resistance genes is denoted by circles for multidrug, squares for beta-lactam, and stars for quinolone ARGs within the respective genera. Additional symbols represent the associated mobile genetic elements (MGEs). The right panel quantifies the relative abundance of each genus, providing insight into their prevalence in the snail gut microbiome

while *Enterobacter* and *Klebsiella* respectively contributed to 9.8% and 6.2% of the multidrug resistance, and 10.3% and 17.2% of the beta-lactam resistance, *Citrobacter* exhibited 33.3% resistance to quinolones. The top 5 genera with the most diverse ARG subtypes are *Pseudomonas* (29 unique subtypes), *Enterobacter* (21 unique subtypes), *Klebsiella* (20 unique subtypes), *Acinetobacter* (19 unique subtypes), and *Citrobacter* (17 unique subtypes) (Table S3).

To validate our metagenomic findings, we isolated and cultured ARBs from snail fecal samples. MIC determination of these isolates revealed high levels of resistance, particularly in genera identified as major ARG hosts in our metagenomic analysis (Table S4). For instance, *Klebsiella pneumoniae* isolates showed MIC values of 128–256 μg/mL for cefotaxime and > 512 μg/mL for ciprofloxacin (Table S4). Similarly, *Pseudomonas* species, including *P. guariconensis* and *P. putida*, exhibited high MICs for both antibiotics, with values ranging from 64 to 128 μg/mL for cefotaxime and 32–64 μg/mL for ciprofloxacin. These results align with our metagenomic data, where *Pseudomonas* and members of Enterobacteriaceae (including *Klebsiella*) were identified as dominant hosts of ARGs.

### Phenotypic responsive antibiotic resistance bacteria

To investigate the active resistome, we analyzed the correlations between resistance phenotypes (i.e., abundance of active ARBs) and the genotypes (i.e., multidrug, betalatame, and quinolone ARGs) at both the contig and MAG level. We observed distinct bacterial responses to two antibiotic resistance phenotypes (Fig. 4). Genera such as *Pantoea*, *Metakosakonia*, *Phytobacter*, *Kosakonia*, and *Enterobacter* showed a significant positive correlation with cefotaxime (beta-lactam) resistance (Fig. 4). In contrast, eight genera, including *Mycobacterium*, *Mycolicibacterium*, *Sphingomonas*, *Rhodanobacter*, *Atlantibacter*, *Kluyvera*, *Shinella*, and *Castellaniella*, showed a weak positive correlation (correlation coefficient > 0.5) with ciprofloxacin resistance (Fig. 4).

Beta-lactam genes were widespread across the studied bacterial genera (Fig. 3), and temperature-dependent variations in bacterial population dynamics were observed. At elevated temperatures, an increase in the prevalence of genera such as *Klebsiella* and *Enterobacter* was noted. We also noted a decrease in the abundance of bacteria harboring quinolone resistance genes (Figs. 3F, 4). In addition, we observed a positive correlation between the abundance of active ARB and ARG-harboring genera (Fig. 4). Multidrug resistance genes, including adeF, baeR, CRP, KpnEHF, and msbA, were prevalent in two types of phenotypic active ARBs (Fig. 4). A diverse array

of beta-lactam genotypes (incl. CGB-1, OmpAK, SHV-1) was associated with the cefotaxime resistance phenotype (Fig. 4). Additionally, cefotaxime phenotype responsive genera contained a higher number of MGEs, such as integrative conjugative elements (ICEs), integrons, and insertion sequences (IS) (Fig. 4).

We obtained 521 high-quality MAGs, with ≥ 90% completeness and ≤ 10% contamination. Our analysis focused on 299 high-quality, ARG-carrying MAGs (spanning 13 phyla, Table S5). These selected MAGs contained a total of 1307 ARGs across 157 distinct subtypes, accounting for half of the total ARG subtypes we identified. Of the high-quality MAGs, 26% had ≥ five ARGs, with 12% carrying ≥ 10 ARGs (Table S5). Of these, 69 and 130 MAGs demonstrated a positive correlation with the abundance of cefotaxime (Fig. 5A) and ciprofloxacin (Fig. 5B) phenotypic resistance level, respectively. Gammaproteobacteria harbored the most ARG-carrying MAGs, and its relative abundance across different temperature treatments surpasses that of the other major ARG-carrying classes (Fig. 5 and Fig. S8). Each ARG-carrying MAGs within Gammaproteobacteria hosted a mean of 7.3 ARGs (14 types and 104 subtypes; more than other dominant phyla, see Table S6). In addition, there were 35 and 44 ARG-carrying high-quality MAGs annotated at the species level, including many opportunistic pathogens (e.g., *Pantoea dispersa*, *Pseudomonas putida*, *Gordonia bronchialis*, *Mycobacterium algericum*; Fig. 5).

### Microbial secondary metabolism in phenotypic responsive antibiotic resistance bacteria

We analyzed the presence and diversity of putative BGCs responsible for the biosynthesis of secondary metabolites, such as antibiotics and siderophores. Among the 299 ARG-carrying MAGs, we identified 235 putative BGCs, with 58 showing 100% similarity (Fig. S9). In contrast, 222 non-ARG carrying MAGs only contain 58 putative BGCs (20 showing 100% identify; Fig. S9).

We then focused specifically on the BGCs within ARG-carrying MAGs that were associated with phenotypic resistance. These BGCs encoded biosynthetic products, predominantly of non-ribosomal peptide synthetases (NPRS, 54), ectoine (52), terpene (19), anylpolyene (18), non-alpha polyamino group acids (NAPAA, 11), and other (19) classes (Fig. S10). Actinobacteria and Gammaproteobacteria were the primary contributors to these BGC types (Fig. S10). We identified a unique specificity in the BGC spectra of bacteria that are resistant to cefotaxime and ciprofloxacin (Fig. S11). Collectively, these MAGs encompassed a total of 44 unique BGCs, seven of which are shared: etoine, carotenoid, ε-poly-L-lysine, flexirubin, myxochelins/pseudochelin, aryl polyenes (APEs), and enterobactin, with ectoine being well distributed phylogenetically. While NRPS types prominently featured in both the cefotaxime and ciprofloxacin-associated MAG groups, their compositions diverged notably (Fig. S11). Specifically, the cefotaxime group contained 11 and the ciprofloxacin group contained 13 of these BGCs, with only myxochelin A/myxochelin B/pseudochelin A being common to both (Fig. S12A–B). A significant portion of ARG-carrying MAGs (ca. one-third, 104 of 299) possessed at least one BGC. This finding indicates a co-occurrence of BGCs and ARGs within these MAGs.

Our investigation of phenotypic resistance identified a subset of 35 MAGs that encode both BGCs and ARGs, which were characterized by their high abundance and positive correlation with rising temperatures (Fig. 6). These MAGs were indicative of temperature-responsive microbes, displaying a genomic predisposition for survival at higher temperatures through the synthesis of protective compounds such as ectoine, xanthomonadin I, and carotenoids, and siderophores like terpenibactin and amonabactin P 750. They also have genes encoding antibiotics and antimicrobial agents, including ε-poly-L-lysine and (Fig. 6).

Of the 20 species-level MAGs (Fig. 6), 13 were identified as opportunistic pathogens, including *Lactococcus lactis* (MAG427), *Pantoea dispersa* (MAG24 and MAG362), *Pseudomonas putid* (MAG3 and MAG 417), and *Gordonia bronchialis* (MAG31, MAG63, MAG117, MAG247, MAG369, and MAG486). In addition to the opportunistic pathogens, strains of *Paenibacillus polymyxa* (MAG363 and MAG25) were noted for their potential competitive advantage at higher temperature treatment (Fig. S12C). These strains harbor genes for the biosynthesis of a variety of antibiotics or antimicrobial substances, such as fusaricidin B, polymyxin, paenila, trideceptin, and paenibacillin, which may contribute to resistance or inhibitory effects against pathogenic bacteria (Fig. 6B).

## Discussion

Climate change, specifically soil warming, is emerging as a critical factor influencing the proliferation of antibiotic resistance in soil-dwelling organisms. In this study, we report a strong correlation between warming and the proliferation of active resistomes in the gut of giant African snails, a globally significant invasive species. We reveal a notable increase in the activity and abundance of ARBs, especially those resistant to multidrug and beta-lactam antibiotics, in response to warming soil temperatures. A concerning interaction between soil warming and the proliferation of active antibiotic resistomes in the gut microbiome of giant African snails, a finding that

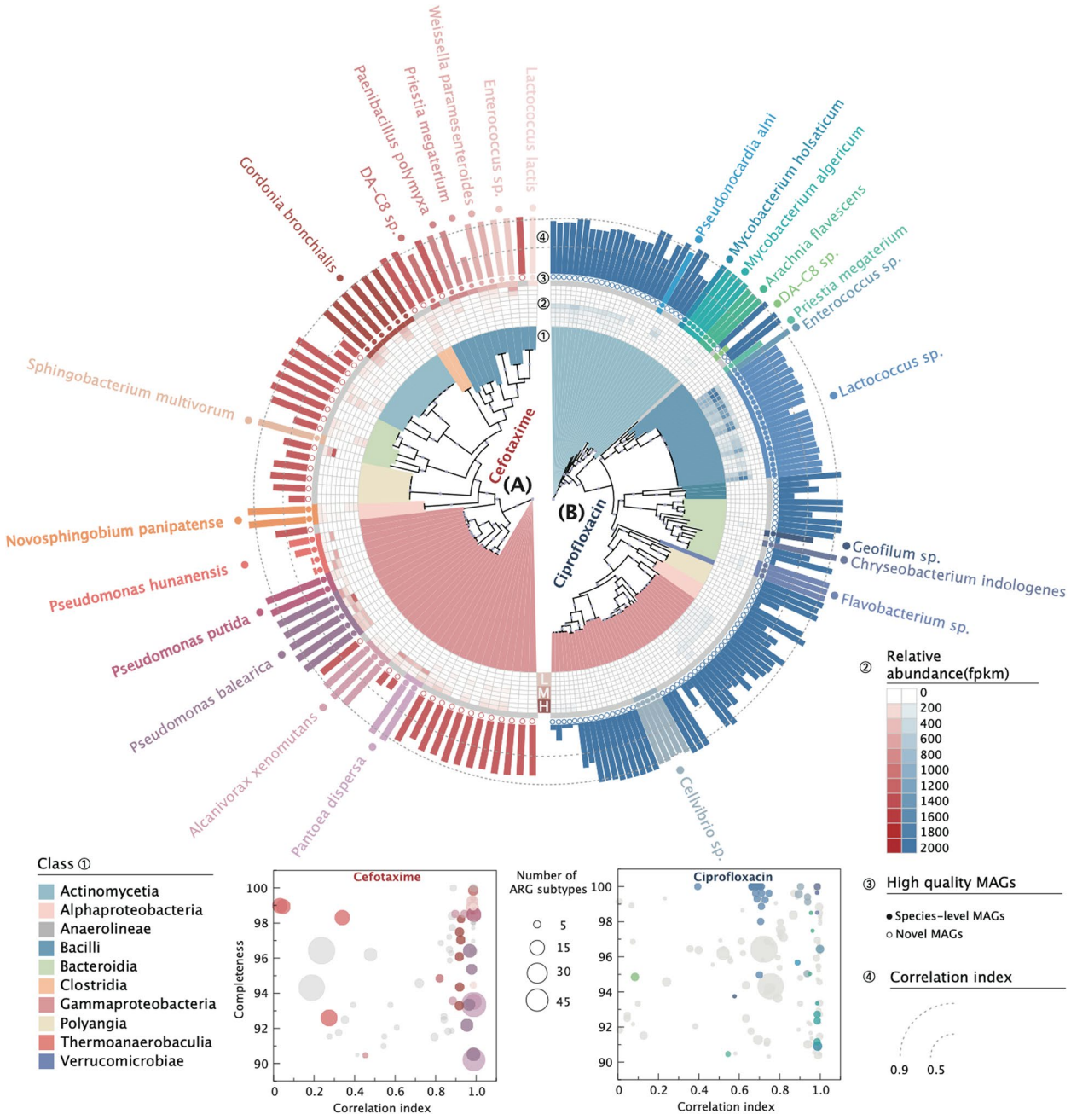


**Fig. 5** Phylogenetic tree of the recovered ARG carrying high-quality MAGs. **A** Phylogenetic tree of cefotaxime resistance MAGs. **B** Phylogenetic tree of ciprofloxacin resistance MAGs. The colors and symbols used in the tree indicate various characteristics of the MAGs. Moving from inside to outside in the colored rings: the first (inner) ring shows a class level taxonomic classification; the second ring (circle heatmap) indicates the relative abundance of each MAGs across various temperature groups (fpkm); the third ring labels species level and novel MAGs; the fourth ring (bar) shows the correlation index (correlations between the relative abundances of each MAG and percentage of phenotypic antibiotic-resistance bacteria)

reflects broader ecological concerns regarding the influence of rising temperatures on AMR [52]. Such advancements expand our understanding of AMR in the face of global warming, highlighting the urgent need to address the potential for soil warming—a direct consequence of climate change—to amplify AMR among soil-dwelling organisms.

We experimentally demonstrate that elevated soil temperatures substantially alter the gut microbiome and resistome of the giant African snail, which subsequently

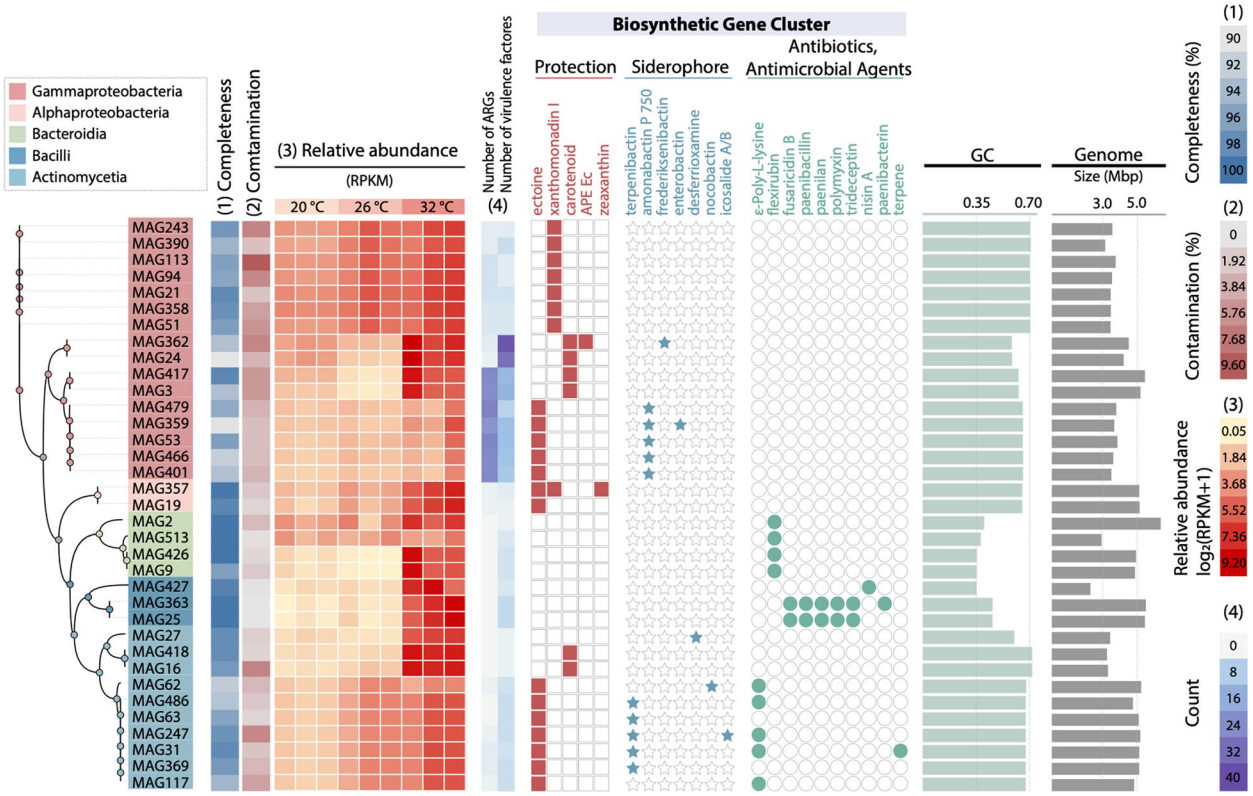


**Fig. 6** Genomic and metabolic profiling of temperature-responsive MAGs with ARG and BGC encoding. Completion (1) and contamination (2) are indicated for each MAG. (3) Heatmap displaying the relative abundance (RPKM) of the selected 35 MAGs across three temperature conditions (20 °C, 26 °C, 32 °C). (4) The number of ARGs of virulence factors is shown alongside the biosynthetic gene clusters (BGCs) involved in protection, siderophore production, and antibiotic biosynthesis. Additional metrics include GC content and genome size (Mbp)

leads to an heightened ARB activity in these snails. First, we observed that increased temperatures induced a gut microbiome imbalance in the giant African snails. A similar phenomenon has been observed in tadpoles, where warming led to dysbiosis of their gut microbiomes and adversely affected their growth [53]. These observations mirror prior research on ectothermic organisms, underscoring that even marginal temperature deviations can elicit physiological stress and heightened mortality, suggesting that even conservative global warming scenarios can have disproportionate impacts on ectothermic species [7].

We observed enhanced activity of ARBs under conditions of elevated soil temperatures, as evidenced by the rising C-D ratio in the single-cell Raman spectra. Furthermore, we found that soil warming increased the abundance of ARB in a certain extent. The combination of single-cell Raman spectroscopy with $D_2O$ labeling has proven instrumental in precisely detecting changes in ARB activity corresponding with temperature fluctuations, aligning with previous research [21]. Therefore, our methodological advancements have thus allowed us to establish a direct link between increased ARB activity and warming soil conditions, further highlighting a notable increase in resistance to beta-lactams within the gut of giant African snails. These collective results not only highlight an increase in ARB activity but also suggest a potential temperature-dependent mechanism at play in AMR. Corroborating our results, a related study on forest soils subjected to simulated climate warming highlighted a significant rise in beta-lactam ARGs due to elevated temperatures [54], thus reinforcing the critical role of temperature in amplifying AMR across various ecosystems. Such findings indicate that rising temperatures may intensify the resistance to certain antibiotics, such as beta-lactams, posing heightened environmental risks in the era of global warming. These findings align with broader concerns about how climate change exacerbates public health challenges [13, 55]. The increased prevalence and activity of ARB under warmer conditions suggests a potential amplification of health risks as global temperatures rise.

Our correlation analysis, which combined Raman-based phenotypes with metagenome-based genotypes,

revealed a significant positive correlation between the abundance of several Enterobacteriaceae family genera (*Pantoea*, *Metakosakonia*, *Phytobacter*, *Kosakonia*, and *Enterobacter*) and active cefotaxime-resistant bacteria. Our results indicate that the Enterobacteriaceae family predominantly hosts multidrug and beta-lactam resistance ARGs, emphasizing the critical role of soil temperature in shaping gut resistance patterns and the propagation of active cefotaxime-resistant bacteria within these genera [56]. Rising global temperatures heighten concerns about increasing ESKAPE pathogens [52]. The prevalence of multiple ARGs and MGEs in ESKAPE pathogens such as *Klebsiella* spp. and *Enterobacter* spp., which flourish at 32 °C in the gut of giant African snails, suggests the potential for enhanced gene transfer mechanisms. The notable ability of ESKAPE pathogens to colonize diverse hosts and transfer resistance genes through horizontal gene transfer (HGT) underlines their significant contribution to the spread of AMR [57–60]. As climate warms, the prevalence and ecological dominance of certain pathogens are likely to increase [61, 62], a trend supported by the identification of numerous potential human pathogens (supercarriers) at the species level within ARG-carrying MAG, which seem to thrive in warmer conditions. Consequently, the adaptability of these human pathogens to warmer conditions, coupled with a broad array of ARGs, presents a formidable challenge in the face of global warming.

We found that ARBs carry a diverse array of BGCs, showcasing a close encoding of ARGs and BGCs within 100 bp to 2 Kb [63]. Microbes employ diverse strategies to adapt to challenging environments, with BGCs playing a crucial role in producing natural products. These products not only facilitate environmental adaptation of microbes and confer competitive advantages, but also broadly contribute to the evolutionary pressures and ecological dynamics shaping ecosystems [64]. Our analysis reveals a functional focus on siderophores, protective compounds, and antimicrobial agents among these ARBs, which are likely crucial for enhancing their environmental adaptability and competitive advantage under environmental stressors [65, 66]. For example, as the most widely distributed protective compounds in warmer temperature-dominant ARBs (Fig. 6), ectoine exemplifies the crucial role of BGCs in enhancing bacterial resilience under environmental stress. It has been reported that ectoine significantly enhances the resilience of bacteria to environmental stresses, particularly with respect to osmotic and heat stress [66]. Our study also highlights the common presence of antioxidant and antimicrobial compounds, including carotenoids, which offer photoprotection and antioxidant properties, and ε-poly-L-lysine, known for its potent antimicrobial activity [67, 68]. This observed co-localization of antimicrobial BGCs and ARGs is consistent with the known imperative for antibiotic-producing organisms to concurrently encode resistance mechanisms as a self-protective strategy [63]. Concurrently, siderophores are crucial for iron uptake, facilitating bacterial survival in iron-scarce environments. Beyond acting as iron carriers, they serve as important mediators between microbial assemblies and their eukaryotic hosts [69]. Additionally, by effectively sequestering iron, siderophores enhance the pathogenicity and competitive advantage of bacteria, playing a pivotal role in their growth and virulence [70]. This discovery underscores the intricate survival strategies of bacteria in warmer conditions, highlighting the sophisticated interplay between antibiotic resistance and microbial competitiveness in changing environments [71, 72].

The intimate genomic association between BGC and ARGs is also exemplified in the non-pathogenic *Paenibacillus polymyxa* (MAG363). This non-pathogen showcases a diverse array of unique BGCs [73], responsible for the synthesis of antimicrobial agents such as fusaricidin B, paenibacillin, paenilan, polymxin, polymyxin, tridecaptin, and paenibacterin, alongside various ARG subtypes (Fig. 6B). The arsenal of antimicrobial activity BGCs endows *P. polymyxa* with a significant competitive edge and heightened adaptability in pathogen-rich environments. This remarkable demonstration of the close linkage between BGCs and ARGs sheds light on the sophisticated survival strategies employed within the snail gut microbiome, particularly in adapting to the challenges posed by escalating soil temperatures.

In conclusion, this work employed both single-cell Raman $D_2O$ and metagenomic sequencing to reveal the dynamics of active AMR in gut microbiome with soil warming. Soil warming increases not only the abundance but also the activity of active ARB. The genotypic analysis further indicated that soil warming accelerated proliferation of ARGs. Notably, we identified specific bacterial taxa, including potential human pathogens, that significantly contribute to the heightened threat of antimicrobial resistance under warmer conditions. Moreover, this study identifies that BGCs render ARBs with a competitive edge under warmer conditions. These findings underscore the adaptive survival strategies within the snail gut microbiome against global climate change, highlighting the urgent need to address the interlinked challenges of climate change and antimicrobial resistance. While our study does not directly demonstrate transmission to local ecosystems or human populations, it highlights the need for continued research on the potential role of invasive species as reservoirs of antibiotic resistance genes under global warming. Nonetheless, this study also underscores the need for future research on in situ investigations that

corroborate these laboratory findings within natural settings, thereby bolstering ecological validity and practical relevance. Taking together, this study provides new understanding regarding soil warming impacts on gut microbiome and AMR of invasive species, and perspectives for future detailed investigations.

## Supplementary Information

The online version contains supplementary material available at https://doi.org/10.1186/s40168-025-02044-7.

Supplementary Material 1.

**Acknowledgements**
Support from Majorbio Company (Shanghai, China) is acknowledged.

**Authors' contributions**
Y.Y.Z., H.Z.L., L.C., X.S., and Y.G.Z. designed the research; Y.Y.Z. and H.Z.L. performed the research; Y.Y.Z. and Z.H.T. analyzed and interpreted the sequencing data and bacterial profiles; M.F.B. and L.C. contributed new analytical methods and insights; Y.Y.Z. wrote the original draft; H.Z.L., M.F.B., X.S., and Y.G.Z. edited the paper; X.S. conceptualized the research and did the funding acquisition. All authors read, edited, and approved the final manuscript.

**Funding**
This work was supported by funds of the National Natural Science Foundation of China (No. 32361143523, 42307165, 42407166), the National Key Research and Development Program of China (No. 2023YFF1304600), the Ningbo S&T project (2021-DST-004), and International Partnership Program of Chinese Academy of Sciences (No. 322GJHZ2022028FN) and the fellowship of China Postdoctoral Science Foundation (No. 2022T150635).

**Data availability**
No datasets were generated or analysed during the current study.

## Declarations

**Ethics approval and consent to participate**
Not applicable.

**Consent for publication**
Not applicable.

**Competing interests**
The authors declare no competing interests.

**Author details**
[1]State Key Laboratory for Ecological Security of Regions and Cities, Ningbo Observation and Research Station, Institute of Urban Environment, Chinese Academy of Sciences, 1799 Jimei Road, Xiamen 361021, People's Republic of China. [2]Zhejiang Key Laboratory of Urban Environmental Processes and Pollution Control, CAS Haixi Industrial Technology Innovation Center in Beilun, Ningbo 315830, People's Republic of China. [3]College of Science & Engineering, Flinders University, Bedford Park, South Australia 5042, Australia. [4]School of Life Sciences, Hebei University, Baoding, 071000 Hebei, People's Republic of China. [5]University of the Chinese Academy of Sciences, 19A Yuquan Road, Beijing 100049, People's Republic of China. [6]Research Center for Eco-Environmental Sciences, Chinese Academy of Sciences, Beijing 100085, People's Republic of China.

Received: 3 June 2024 Accepted: 20 January 2025
Published online: 06 February 2025

**References**

1. Melillo J, et al. Soil warming and carbon-cycle feedbacks to the climate system. Science. 2002;298(5601):2173–6.
2. Wardle DA, et al. Terrestrial ecosystem responses to species gains and losses. Science. 2011;332(6035):1273–7.
3. Sinclair BJ, et al. Can we predict ectotherm responses to climate change using thermal performance curves and body temperatures? Ecol Lett. 2016;19(11):1372–85.
4. Wu L, et al. Reduction of microbial diversity in grassland soil is driven by long-term climate warming. Nat Microbiol. 2022;7(7):1054–62.
5. Yuan MM, et al. Climate warming enhances microbial network complexity and stability. Nat Clim Chang. 2021;11(4):343–8.
6. Coyle DR, et al. Soil fauna responses to natural disturbances, invasive species, and global climate change: current state of the science and a call to action. Soil Biol Biochem. 2017;110:116–33.
7. Jørgensen LB, et al. Extreme escalation of heat failure rates in ectotherms with global warming. Nature. 2022;611(7934):93–8.
8. Abram PK, et al. Behavioural effects of temperature on ectothermic animals: unifying thermal physiology and behavioural plasticity. Biol Rev. 2017;92(4):1859–76.
9. Wright GD. The antibiotic resistome: the nexus of chemical and genetic diversity. Nat Rev Microbiol. 2007;5(3):175–86.
10. Xiang Q, et al. Microbial multitrophic communities drive the variation of antibiotic resistome in the gut of soil woodlice (Crustacea: Isopoda). Environ Sci Technol. 2022;56(21):15034–43.
11. Zhang Y, et al. Increasing antimicrobial resistance and potential human bacterial pathogens in an invasive land snail driven by urbanization. Environ Sci Technol. 2023;57(18):7273–84.
12. Bei Q, Thomas R, Beatrix S, Nico E, Martin S, François B, and Anna HB. Extreme summers impact cropland and grassland soil microbiomes. The ISME Journal. 2023;17(10):1589–1600. https://doi.org/10.1038/s41396-023-01470-5
13. Singh BK, Manuel DB, Eleonora E, and Philip GT. Climate change impacts on plant pathogens, food security and paths forward. Nature Reviews Microbiology. 2023;21(11):640–656. https://doi.org/10.1038/s41579-023-00900-7
14. Kohl KD, Yahn J. Effects of environmental temperature on the gut microbial communities of tadpoles. Environ Microbiol. 2016;18(5):1561–5.
15. Murray CJ, et al. Global burden of bacterial antimicrobial resistance in 2019: a systematic analysis. The Lancet. 2022;399(10325):629–55.
16. Wang L, et al. The pH-specific response of soil resistome to triclocarban and arsenic co-contamination. J Hazard Mater. 2024;464:132952.
17. Abiona JA, et al. Comparative evaluation of haemagglutination potential of haemolymph from two species of giant African land snails (Archachatina marginata and Achatina achatina). Fish Shellfish Immunol. 2014;38(1):96–100.
18. Rekha Sarma, R., M. Munsi, and A. Neelavara Ananthram, Effect of climate change on invasion risk of giant African snail (Achatina fulica Férussac, 1821: Achatinidae) in India. PLoS One. 2015;10(11):e0143724.
19. Song J, et al. Carbendazim shapes microbiome and enhances resistome in the earthworm gut. Microbiome. 2022;10(1):63.
20. Luo F, et al. Network complexity of bacterial community driving antibiotic resistome in the microbiome of earthworm guts under different land use patterns. J Hazard Mater. 2024;461:132732.
21. Li H-Z, et al. Active antibiotic resistome in soils unraveled by single-cell isotope probing and targeted metagenomics. Proc Natl Acad Sci. 2022;119(40):e2201473119.
22. Carini P, et al. Relic DNA is abundant in soil and obscures estimates of soil microbial diversity. Nat Microbiol. 2016;2(3):1–6.
23. Wang D, et al. Advances in single cell Raman spectroscopy technologies for biological and environmental applications. Curr Opin Biotechnol. 2020;64:218–29.
24. Li H-Z, et al. Phenotypic tracking of antibiotic resistance spread via transformation from environment to clinic by reverse D2O single-cell Raman probing. Anal Chem. 2020;92(23):15472–9.
25. Wang Y, et al. Raman-activated sorting of antibiotic-resistant bacteria in human gut microbiota. Environ Microbiol. 2020;22(7):2613–24.
26. Srivastava PD. Problem of land snail pests in Agriculture: A study of the giant African snail. Dehradun:Concept Publishing Company. 1992. [Book]
27. Albuquerque, F.S.d., et al., Do climate variables and human density affect Achatina fulica (Bowditch) (Gastropoda: Pulmonata) shell length,

total weight and condition factor? Brazilian Journal of Biology, 2009;69: 879–885.
28. Borchardt MA, et al. The environmental microbiology minimum information (EMMI) guidelines: qPCR and dPCR quality and reporting for environmental microbiology. Environ Sci Technol. 2021;55(15):10210–23.
29. Callahan BJ, et al. DADA2: high-resolution sample inference from Illumina amplicon data. Nat Methods. 2016;13(7):581–3.
30. Bolyen E, et al. Reproducible, interactive, scalable and extensible microbiome data science using QIIME 2. Nat Biotechnol. 2019;37(8):852–7.
31. Andrews, S., FastQC: a quality control tool for high throughput sequence data. 2010, Babraham Bioinformatics, Babraham Institute, Cambridge, United Kingdom.
32. Bolger AM, Lohse M, Usadel B. Trimmomatic: a flexible trimmer for Illumina sequence data. Bioinformatics. 2014;30(15):2114–20.
33. Langmead B, Salzberg SL. Fast gapped-read alignment with Bowtie 2. Nat Methods. 2012;9(4):357–9.
34. Yin X, Ying Yang UM, and Thomas UB. ARGs-OAP v3. 0: Antibiotic-resistance gene database curation and analysis pipeline optimization. Engineering. 2023;19(2):234–41. https://doi.org/10.1016/j.eng.2022.10.011
35. Alneberg J, et al. Binning metagenomic contigs by coverage and composition. Nat Methods. 2014;11(11):1144–6.
36 Wu YW, Simmons BA, Singer SW. MaxBin 2.0: an automated binning algorithm to recover genomes from multiple metagenomic datasets. Bioinformatics. 2016;32(4):605–7.
37. Kang DD, et al. MetaBAT 2: an adaptive binning algorithm for robust and efficient genome reconstruction from metagenome assemblies. PeerJ. 2019;7:e7359.
38. Parks DH, et al. CheckM: assessing the quality of microbial genomes recovered from isolates, single cells, and metagenomes. Genome Res. 2015;25(7):1043–55.
39. Chaumeil PA, Aaron JM, Philip H, and Donovan HP. GTDB-Tk: a toolkit to classify genomes with the Genome Taxonomy Database. Bioinformatics. 2020;36(6):1925–7. https://doi.org/10.1093/bioinformatics/btz848
40. Price MN, Dehal PS, Arkin AP. FastTree 2–approximately maximum-likelihood trees for large alignments. PLoS ONE. 2010;5(3): e9490.
41. Letunic I, Bork P. Interactive Tree Of Life (iTOL) v4: recent updates and new developments. Nucleic Acids Res. 2019;47(W1):W256–9.
42. Blin, K., et al., antiSMASH 6.0: improving cluster detection and comparison capabilities. Nucleic acids research, 2021. 49(W1): p. W29-W35.
43. Lin D, et al. Long-term application of organic fertilizer prompting the dispersal of antibiotic resistance genes and their health risks in the soil plastisphere. Environ Int. 2024;183:108431.
44. Yin X, Xi Chen Xiao-Tao J, Ying Y, Bing L, Marcus Ho-Hin S, Tommy TY Lam et al. Toward a universal unit for quantification of antibiotic resistance genes in environmental samples. Environmental Science & Technology. 2023;57(26):9713–21. https://doi.org/10.1021/acs.est.3c00159
45. Schoch, C.L., et al., NCBI Taxonomy: a comprehensive update on curation, resources and tools. Database, 2020. 2020: p. baaa062.
46. Zhang Z, Zhang G, Ju F. Using culture-enriched phenotypic metagenomics for targeted high-throughput monitoring of the clinically important fraction of the β-lactam resistome. Environ Sci Technol. 2022;56(16):11429–39.
47. Rice EW, et al. Determining hosts of antibiotic resistance genes: a review of methodological advances. Environ Sci Technol Lett. 2020;7(5):282–91.
48. Institute, C.a.L.S., Methods for dilution antimicrobial susceptibility tests for bacteria that grow aerobically, 11th edition CLSI standard M07. 2018, Wayne, PA: Clinical and Laboratory Standards Institute.
49. Institute, C.a.L.S., Performance standards for antimicrobial susceptibility testing, 32nd edition CLSI supplement M100. 2022, Wayne, PA: Clinical and Laboratory Standards Institute.
50. R Core Team. R: A language and environment for statistical computing. R Foundation for Statistical Computing, Vienna, Austria. 2021. https://www.R-project.org/
51. Liu C, et al. microeco: an R package for data mining in microbial community ecology. FEMS microbiology ecology. 2021;97(2):255.
52. MacFadden DR, et al. Antibiotic resistance increases with local temperature. Nat Clim Chang. 2018;8(6):510–4.
53. Greenspan SE, et al. Warming drives ecological community changes linked to host-associated microbiome dysbiosis. Nat Clim Chang. 2020;10(11):1057–61.
54. Li Z, et al. Climate warming increases the proportions of specific antibiotic resistance genes in natural soil ecosystems. J Hazard Mater. 2022;430:128442.
55. Mora C, et al. Over half of known human pathogenic diseases can be aggravated by climate change. Nat Clim Chang. 2022;12(9):869–75.
56. Romero GQ, et al. Global predation pressure redistribution under future climate change. Nat Clim Chang. 2018;8(12):1087–91.
57. de Sousa JM, Lourenço M, Gordo I. Horizontal gene transfer among host-associated microbes. Cell Host Microbe. 2023;31(4):513–27.
58. Wyres KL, Holt KE. Klebsiella pneumoniae as a key trafficker of drug resistance genes from environmental to clinically important bacteria. Curr Opin Microbiol. 2018;45:131–9.
59. De Oliveira DM, et al. Antimicrobial resistance in ESKAPE pathogens. Clin microbiol rev. 2020;33(3):e00181-19.
60. Ni B, et al. Effects of heavy metal and disinfectant on antibiotic resistance genes and virulence factor genes in the plastisphere from diverse soil ecosystems. J Hazard Mater. 2024;465:133335.
61. McKenzie T, Gaw IM. Climate change exacerbates almost two-thirds of pathogenic diseases affecting humans. Berlin, 14197, Germany: Heidelberger Platz 3; 2022. p. 791–791.
62. Elderd BD, Reilly JR. Warmer temperatures increase disease transmission and outbreak intensity in a host–pathogen system. J Anim Ecol. 2014;83(4):838–49.
63. Busi SB, et al. Glacier-fed stream biofilms harbor diverse resistomes and biosynthetic gene clusters. Microbiology Spectrum. 2023;11(1):e04069-e4122.
64 Dong X, et al. A vast repertoire of secondary metabolites potentially influences community dynamics and biogeochemical processes in cold seeps. Science Advances. 2024;10(17):eadl2281.
65. Dove NC, Taş N, Hart SC. Ecological and genomic responses of soil microbiomes to high-severity wildfire: linking community assembly to functional potential. ISME J. 2022;16(7):1853–63.
66. Pastor JM, et al. Ectoines in cell stress protection: uses and biotechnological production. Biotechnol Adv. 2010;28(6):782–801.
67. Bo T, et al. Metabolomic analysis of antimicrobial mechanisms of ε-poly-l-lysine on Saccharomyces cerevisiae. J Agric Food Chem. 2014;62(19):4454–65.
68. Stahl W, Sies H. Antioxidant activity of carotenoids. Mol Aspects Med. 2003;24(6):345–51.
69. Kramer J, Özkaya Ö, Kümmerli R. Bacterial siderophores in community and host interactions. Nat Rev Microbiol. 2020;18(3):152–63.
70. Behnsen J, et al. Siderophore-mediated zinc acquisition enhances enterobacterial colonization of the inflamed gut. Nat Commun. 2021;12(1):7016.
71. Bruns H, et al. Function-related replacement of bacterial siderophore pathways. ISME J. 2018;12(2):320–9.
72. Heilbronner S, et al. The microbiome-shaping roles of bacteriocins. Nat Rev Microbiol. 2021;19(11):726–39.
73. Liu L, et al. Charting the complexity of the activated sludge microbiome through a hybrid sequencing strategy. Microbiome. 2021;9:1–15.

## Publisher's Note